Computers & Graphics 37 (2013) 225–237

Contents lists available at SciVerse ScienceDirect

Computers & Graphics

journal homepage: www.elsevier.com/locate/cag

Special Section on Procedural Modeling

Procedural grape bunch modeling

Chun-Yen Huang [a], Wan-Ting Jheng [a], Wen-Kai Tai [a,*], Chin-Chen Chang [b], Der-Lor Way [c]

[a] Department of Computer Science and Information Engineering, National Dong Hwa University, Hualien, Taiwan
[b] Department of Computer Science and Information Engineering, National United University, Miao-Li, Taiwan
[c] School of Film and New Media, Taipei National University of the Arts, Taipei, Taiwan

ARTICLE INFO

Article history:
Received 2 August 2012
Received in revised form
20 December 2012
Accepted 3 January 2013
Available online 23 January 2013

Keywords:
Procedural modeling
Grammar-based approach
Open L-system
Grape bunch

ABSTRACT

This paper proposes a grammar-based procedural approach for modeling of grape bunches. A proposed description of the formal rules of an open L-system can be used to model almost all types of grape bunches. When growing a grape bunches, the overall shape for controlling the development is first given by users through the provided user interface, which determines the parameters used for rules. The interaction simulation process then simulates the natural thinning effect between the newborn internode and the existing grape structure via a communication module for the adjustment of the growing directions of branches, twigs and berries during the interpretation of generated string. As experimental results show, our approach is capable of modeling almost all types of grape bunches effectively with realistic visual effects. Also, our approach can be extended to modeling many panicle berry bunches.

1. Introduction

The power of the procedural approach for modeling 3D objects is about its flexibility. In recent years, many grammar-based procedural modeling approaches have been proposed for plants [1], buildings [2], natural phenomena [3], etc. However, the gap between formal rules' descriptions and development's controls of procedural models is not easy to be overcome, making their applications limited [4]. In this paper, we aim to propose a description of formal rules to model grape bunches and control the development of the proposed grammar-based procedural method through intuitive user interactions.

According to the statistical data of the Food and Agriculture Organization (FAO) of the United Nations [5], the grape has the largest production value of any fruit in the world. Grape bunches have been seen commonly around our life not only as food, but also as decorations. In addition, the digital content of grape bunches is required in many applications such as movies, games and animation. Existing grammar-based plant approaches [6–9] are not suitable or easy to adapt for modeling various types of grape bunch. To account for modeling grape bunches, two major characteristics – thinning and bottom-up interpretation – must be considered. Thinning means to reduce the number of berry in a bunch, occurs by methods of natural withering such as wind, limitation of growing space, etc., or manual thinning by farmers. Bottom-up interpretation is to interpret the string of L-system from leaves to root of the branching structure.

We propose a modeling process based on an open L-system to model grape bunches by simulating the interactions between branches/twigs and berries. The *communication module* helps the system to adjust the growing direction of branches, twigs and berries when developing the bunch model. This simulation process makes natural withering possible. We have also implemented an interface for users to interactively control the approximate shape of the berry bunch by profiling the bunch with an eight-face polyhedron. With this interface, manual thinning can be achieved through users' adjustment. The orders of the symbols in the final L-system are organized for the depth-first developing so that the string interpretation is bottom-up, making the simulation process of the environment interactions efficient.

The resulting 3D berry bunch model can be exported for further applications. Fig. 1 provides the overview of the proposed system and an example of the comparison between the rendered grape bunch modeled by our system and the real one. The experimental results show that the proposed approach is capable of modeling the common berry bunch without unnatural space or overlapping between berries, which is a great help for berry bunch modeling. The results also show that the user interface is sufficient to control the shape of the bunch. Furthermore, the results also show that our approach can be applied to model several different kinds of panicle berry bunch as well.

The rest of the paper is organized as follows. In Section 2, we briefly review the related work on the L-system and its applications. The characteristics of the grape bunch are described in Section 3. The method is discussed in Section 4. Implementation and results are in Section 5, and the paper is concluded in Section 6 with the discussion of future work.

* Corresponding author. Tel.: +886 3 8634023; fax: +886 3 8634010.
E-mail addresses: wenkaitai@gmail.com, wktai@mail.ndhu.edu.tw (W.-K. Tai).

0097-8493/$ - see front matter
http://dx.doi.org/10.1016/j.cag.2013.01.002

Fig. 1. System overview (left). Real grape bunch (middle). Exported 3D model rendered by MAYA with subsurface scattering (right).

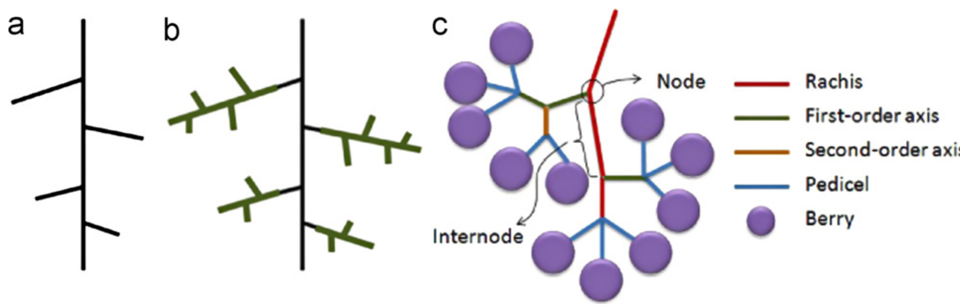

Fig. 2. A 2D structure example of inflorescence and a grape bunch: (a) raceme, (b) panicle and (c) grape bunch. (For interpretation of the references to color in this figure caption, the reader is referred to the web version of this article.)

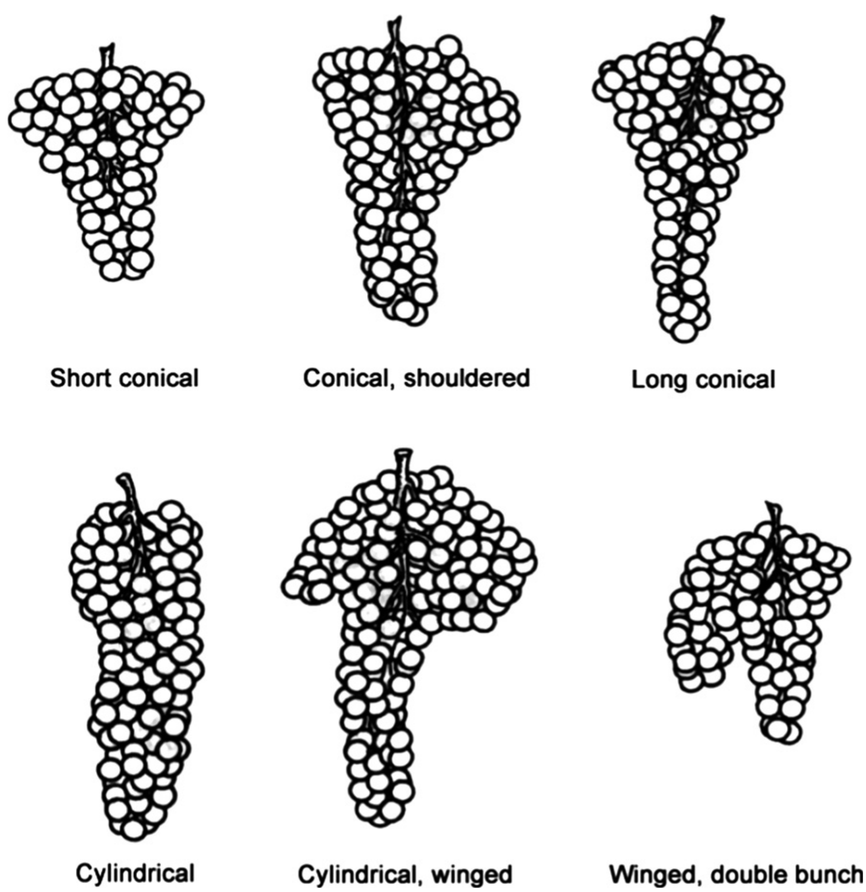

Fig. 3. The six shape types of grape bunch.

2. Related work

For the last few decades, many procedural modeling techniques have been developed and proven to be valuable in very diverse domains of computer graphics [10]. Most of them are targeted toward modeling a specific type of object or environment. Examples include plant modeling [1], ecosystem modeling [11], river modeling [12], buildings modeling [2], textures synthesizing [13] feather modeling [14], and icicle modeling [3].

For the modeling of building, procedural methods build 3D architecture models from rules and shape grammars. These methods generate highly detailed 3D architecture models on the scale of both an individual building [2] and an entire city [15]. The disadvantages of these methods are (a) it takes expertise for effective use and (b) it is difficult to specify rules to model a particular building.

For the modeling of plants, Prusinkiewicz and Lindenmayer first showed that plausible results can be achieved by using L-systems [1]. Researchers also successfully achieved impressive results on plants by simulating growth in open space using an L-system [16–18,8]. An L-system is a parallel rewriting system where modules are rewritten by means of production rules to produce a complex object that with self-similarity.

Měch and Prusinkiewicz extended L-system to consider how plants interact with their environment as they grow and proposed an open L-system [6]. An open L-system adds the plant–environment interaction as a *communication module* based on an L-system for simulating the behavior between plant and environment. The *communication module* $?E(p_0,p_1,\ldots,p_m)$ sets the parameters p_i by values obtained from the environment. An example is module $?E(d)$ that measures the distance to an obstacle. The actual semantics of each *communication module* are defined by the designer of the L-system. Such an idea has also been applied to urban space modeling [15].

Jirasek et al. [19] presented a developmental plant models expressed using L-systems. The model captured impact of gravity, tropisms, contact between elements of a plant structure and contact with obstacles on the shape of branches, into L-system-based models. Although this approach was referring to the modeling of grape bunches, the details of the L-system model were not described. Besides, users are unable to control the resulting shape for producing the different types of grape bunch.

Prusinkiewicz et al. [20] employed a given silhouette to constrain the generated branching structure based on L-system. Users can obtain the desired resulting shape easily with the silhouette. We take this idea in the proposed approach with the open L-system to approximate the physically based simulated method, producing plausible results.

Table 1
Turtle interpretation of the modules.

Module	Interpretation
$F(s)$	Move ahead s and draw a line with length s
$S(i)$	Move ahead i and draw a sphere with radius i
$+(\theta)$	Rotate θ with axis U clockwise
$-(\theta)$	Rotate θ with axis U counter-clockwise
$\&(\theta)$	Rotate θ with axis L clockwise
$\wedge(\theta)$	Rotate θ with axis L counter-clockwise
$/(\theta)$	Rotate θ with axis H clockwise
$\backslash(\theta)$	Rotate θ with axis H counter-clockwise
$!(w)$	Set the line width to w
[	Push present state to the stack
]	Pop a state from the stack
%	Remove the following symbol(s)

The default angle of the rotation module is 90°.

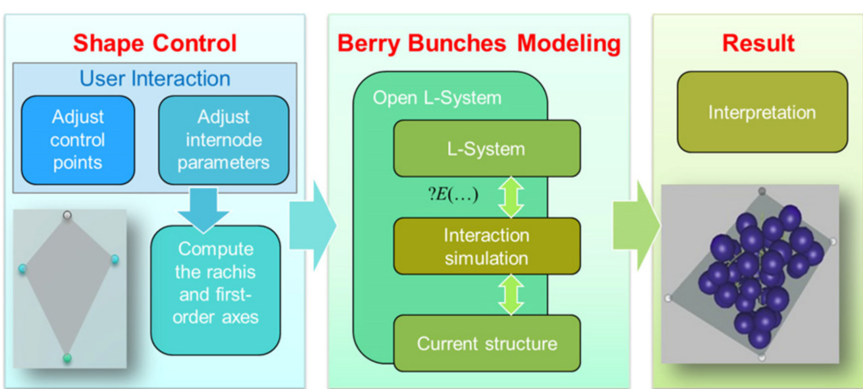

Fig. 4. Framework of the grape bunches modeling.

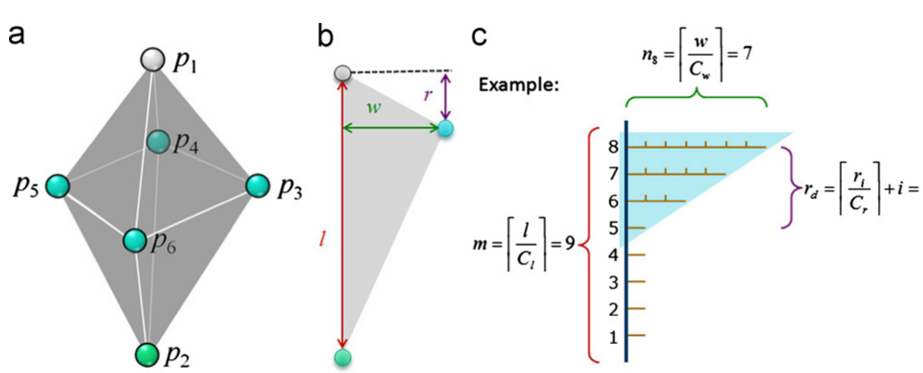

Fig. 5. An illustration of profiling the grape bunch. (a) Using a polyhedron to profile the shape of a grape bunch, (b) segment computation of rachis and first-order axes and (c) an example of profiling a grape bunch.

3. Grape bunch

This section describes the general structure of a grape bunch [21,22]. The inflorescence of a grape plant is panicle [23]. A panicle is a branched bunch of flowers in which the branches are racemes; in other words, a compound raceme [24,25]. Fig. 2(a) and (b) shows a 2D structure example of these two kinds of inflorescences. The green parts in Fig. 2(b) are racemes. The blooming order of flower buds starts from the middle of a bunch, followed by the base, and finally the tip [26,27]. The number of the buds in a bunch is different depending on the species and ages of the grape [26]. There are 200–500 buds in a bunch, and 1500 at most [26]. However, only 20–30 berries or so will be left after thinning [26]. The shapes of bunches are classified into six types: short conical, shouldered conical, long conical, cylindrical, winged cylindrical, and double bunch winged [28] as shown in Fig. 3. The internode that connects the berry is also called a pedicel [29]. Fig. 2(c) shows a 2D structure example of a grape bunch.

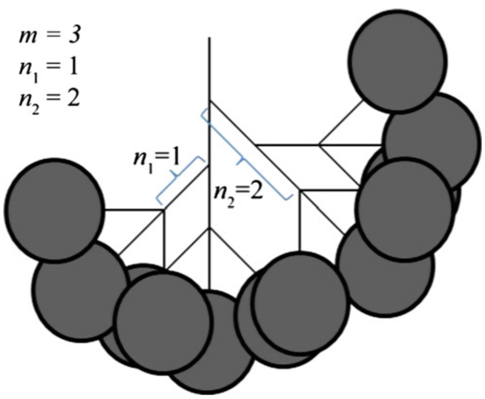

Fig. 6. An example of the interpreted result of basic L-system.

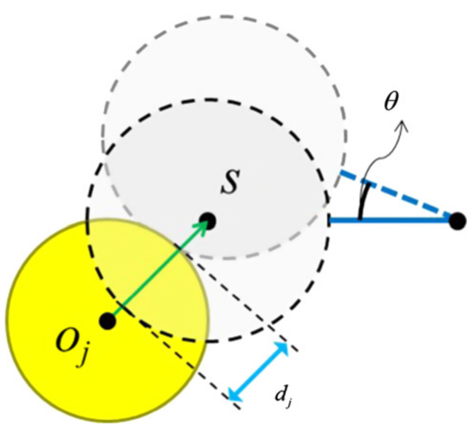

Fig. 7. Pushing force and the rotation angle θ in 2D representation.

4. Procedural grape bunch modeling

4.1. Overview

The shape of a grape bunch is formed by the berries, while the growing directions and positions of each berry are decided by the innate branching pattern of inflorescence. However, the volume and weight of each berry itself will change the position of other berries via pushing and collision between berries when growing, and will also affect the twigs that connect the berries. Therefore, we use an open L-system to simulate such self-interacted activity.

Fig. 4 shows the framework of the proposed approach. There are three stages in the growing process of the grape bunch. First, the rough shape of the grape bunch should be decided. Users can drag the control points to obtain the shape of the grape because our approach initially generates a grape bunch from the default parameters. The parameters of rachis and first-order axes $(m,n_{1\ldots m-1})$ are then computed. Second, the open L-system grows the bunch with the parameters by iteratively simulating the interaction and growing of the self-structure of the grape bunch. In the third stage, the final result is obtained after finishing the interpretation.

4.2. Profiling the grape bunch

The shape form of a grape bunch can be profiled using a polyhedron with eight faces, an octahedral form of three polytopes. To guide the growing simulation of the proposed L-system

Table 2
The execution times with different number of internodes and berries.

Internodes	Berries	Time (in ms)
179	41	610
177	53	697
177	75	816
178	82	831
172	102	919
183	110	1009
197	118	1108

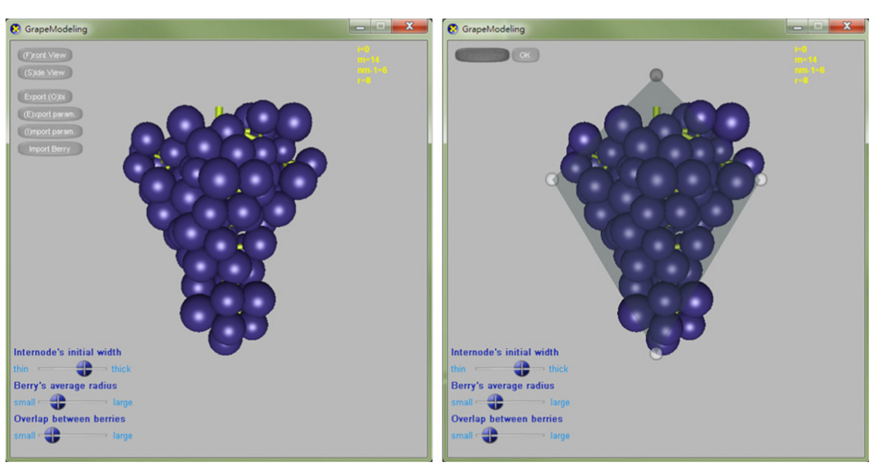

Fig. 8. User interface. Interface overview (left) and front view of control point interface (right).

specified below, we provide a friendly interaction environment to users where they can quickly determine the approximate shape form by profiling an octahedral form. As few as six control points are sufficient to control the profile of a grape bunch. As shown in Fig. 5(a), the fixed reference points p_1 and bottom control point p_2 are used to determine the length of rachis (l), and four side control points, p_3–p_6, control the width (w) of the irrespective first-order axes. Using an eight-face polyhedron aligns the control points p_3, p_5 and p_4, p_6 with the front view and side view, respectively, for user-friendly adjustment of the control points in 2D mode.

When the grape bunch has been profiled, we determine the parameters required to grow the grape bunch in the proposed L-system. In general, the number of segments (m) of the rachis is proportional to the length of the grape bunch, and is defined as $m=\lceil l/C_l \rceil$, where C_l is a constant that transforms the screen space distance to the rachis segments as shown in Fig. 5(b). Also, we define the number of segments ($n_s, s=1\ldots m-1$) of the longest first-order axis by $n_s=\lceil w/C_w \rceil$, where C_w is a constant that transforms the screen space distance to the longest first-order axis segments. The number of segments for each first-order axis decreases linearly from the top first-order axis to the last one. The decreasing rate of the first order axes is defined by $r_d=\min(\lceil r_i/C_r \rceil+i, m-1)$ where r_i is the height difference between the fixed reference point p_1 and the side control point p_i, C_r is a constant that transforms the screen space distance to the decreasing rate of the first order axes, and i is the index of the side control point. Fig. 5(c) illustrates an example of the calculation for these parameters with $m=9$, $n_8=7$, and $r_d=4$ in a single side.

4.3. Grape bunch modeling

The grape bunch grows over time and will be shaped by thinning naturally; a result of an intra-interaction. We use the open L-system to simulate the intra-bunch interaction. There are four parts of the original structure of the open L-system [6]: plant model, plant simulation, environment analysis and environment information. Plant model is the original L-system. Due to the considered external force of a grape bunch being only the interaction of collisions between the berries, which is not necessarily separated into plant and environment process, we thus simplify and combine the plant simulation and environment analysis of the open L-system into an interaction simulation process. The current structure is the same as the environment information of the original open L-system which includes the element information of internode and berry when growing. The *communication module* $?E(\ldots)$ passes the growing information, such as original direction and position, to the interaction simulation process. By querying the current structure, the interaction simulation process can get the information of the nearby obstacles (berries/internodes) and then adjust the growing direction of the newborn branch. After the growing direction is corrected, the L-system is updated through the *communication module* and the information in current structure is updated as well by the interaction simulation.

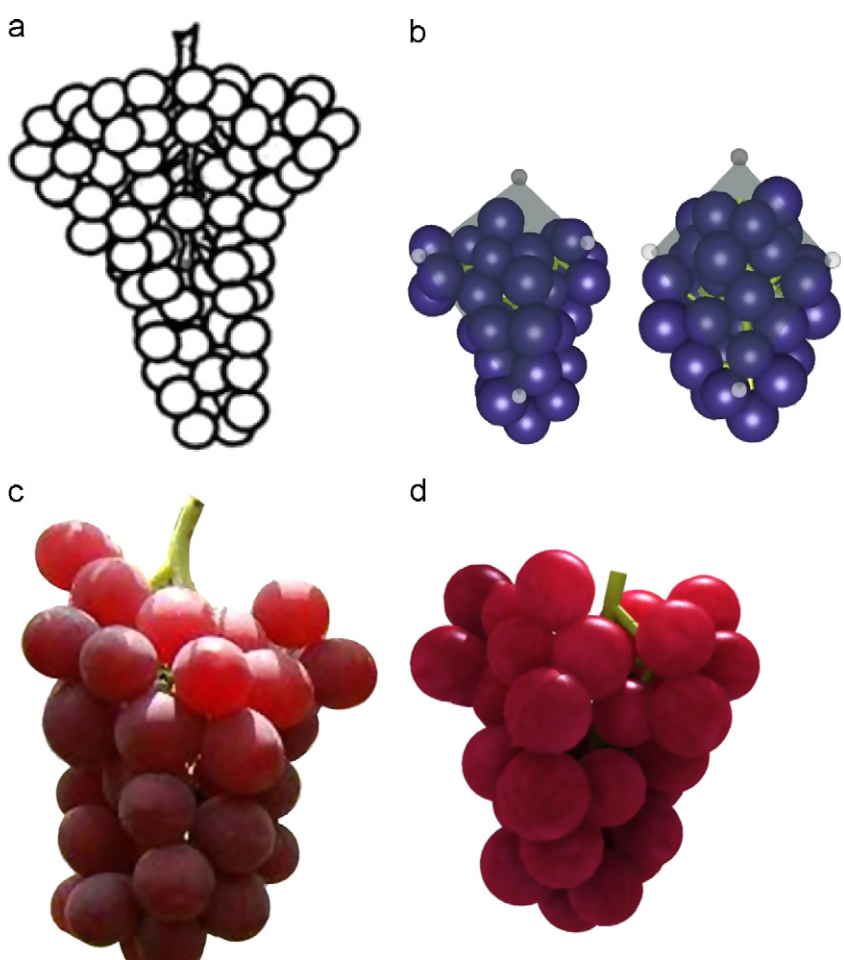

Fig. 9. Short conical of grape bunch. (a) Sample shape illustration, (b) front and side views of the shape control result, (c) real grape bunch and (d) rendered result.

The following will first describe the traditional L-system and indicate what problems will occur without a *communication module*, and then the advantages of a complete open L-system with a *communication module* will be introduced. The symbols of turtle interpretation we used are shown in Table 1.

4.3.1. Basic L-system

The inflorescence of a grape bunch is a compound raceme that is formed by three elements: rachis, first-order axis, and second-order axis. The development is ended with end structure (pedicel and berry). We explain the development of the inflorescence first with a 2D example and then in three dimensions. The following L-system 1 grows the basic grape bunch in 2D.

L-system 1. The basic L-system of a grape bunch.

Input
m : number of derivation steps for rachis.
$n_1 \ldots n_{m-1}$: number of derivation steps for first-order axes.

#define l 60 /* internode's initial length */
#define r_l 1 /* internode's length decreasing rate */
#define r_r 0.75 /* the ratio of sphere's radius to internode's initial length*/
#define α 45 /* yaw angle */

$\omega : A_r(m,l)$
$p_1 : A_r(i,j) : i>1 \rightarrow F(j)[//A_r(i-1,j*r_l)][+(\alpha)A_f(n_{i-1},j*r_l)]$
$p_2 : A_r(i,j) : i==1 \rightarrow A_e(j*r_l)$
$p_3 : A_f(i,j) : i>1 \rightarrow F(j)[//A_f(i-1,j*r_l)][+(\alpha)A_e(j*r_l)]$
$p_4 : A_f(i,j) : i==1 \rightarrow A_e(j*r_l)$
$p_5 : A_e(i) \rightarrow F(i)[A_p(i*r_l)][+(\alpha)A_p(i*r_l)][-(\alpha)A_p(i*r_l)]$
$p_6 : A_p(i) \rightarrow F(i)S(l*r_r)$

A_r, A_f, A_e, and A_p represent the apex symbols of rachis, first-order axis, end structure, and pedicel respectively. The axiom ω represents the initial apex of a rachis with two parameters: the number of segments in the rachis, m, and internode, l. The feature of the panicle is that the development of the rachis and first-order axis is similar, which grows an internode with an apex and then creates a new branch. Rules p_1 and p_3 correspond to the growing behavior of the rachis and first-order axis respectively while rules p_2 and p_4 are used to grow the end structure. There are usually three flower buds at the end of the twig, and thus the end structure will create three branches of pedicel apex after growing

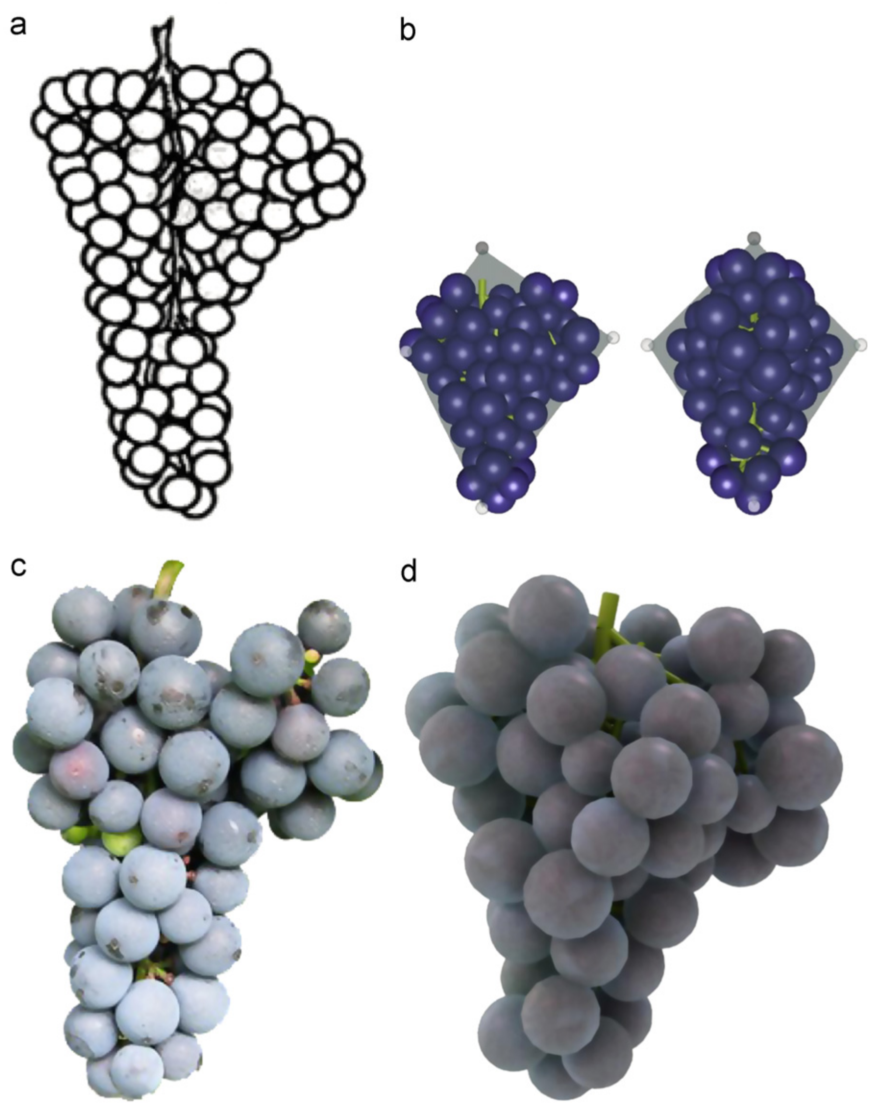

Fig. 10. Shouldered conical of grape bunch. (a) Sample shape illustration, (b) front and side views of the shape control result, (c) real grape bunch and (d) rendered result.

an internode in rule p_5. Rule p_6 then creates an internode with a sphere to represent the berry. Note that the default value of rotation angle is set to be 90°.

Fig. 6 shows an example of the interpreted result of a basic L-system with $m=3$, $n_1=1$, and $n_2=2$ as input parameters. The overlapped berries are obtained due to the lack of growing direction correction in the basic L-system. Note that the number of derivation steps for all first-order axes $0,1,\ldots,m-1$ is determined by the method previously described in Section 4.1.

4.3.2. Open L-system

The open L-system is to simulate the interaction between the newborn structure (internodes and berries) and current structure when growing. The interaction simulation will adjust the growing direction downward to approximate the effect of gravity or evade crowded spaces.

Thinning is also an important process when growing; artificial thinning is performed for berries if the space is too crowded to increase the berries' sizes and their sweetness. There is natural thinning as well due to the fact that the wind or rain may make berries drop. The proposed interaction simulation process of the open L-system is able to simulate thinning when growing the grape bunch. The pedicel will be withered and the following berry will be canceled if there still exist collisions after adjusting the growing direction many times.

The order of the symbol decides the order of the string interpretation. We expect the depth-first developing order, so the rachis symbol is placed at the left of the branching symbol. This makes the string interpretation bottom-up, which is easier for approximation of the gravity effect.

The following L-system 2 shows the improved L-system with *communication module* $?E(\ldots)$. The differences to the basic L-system are marked in bold.

L-system 2. The open L-system of the grape bunch improved from L-system 1.

Input
m : number of derivation steps for rachis.

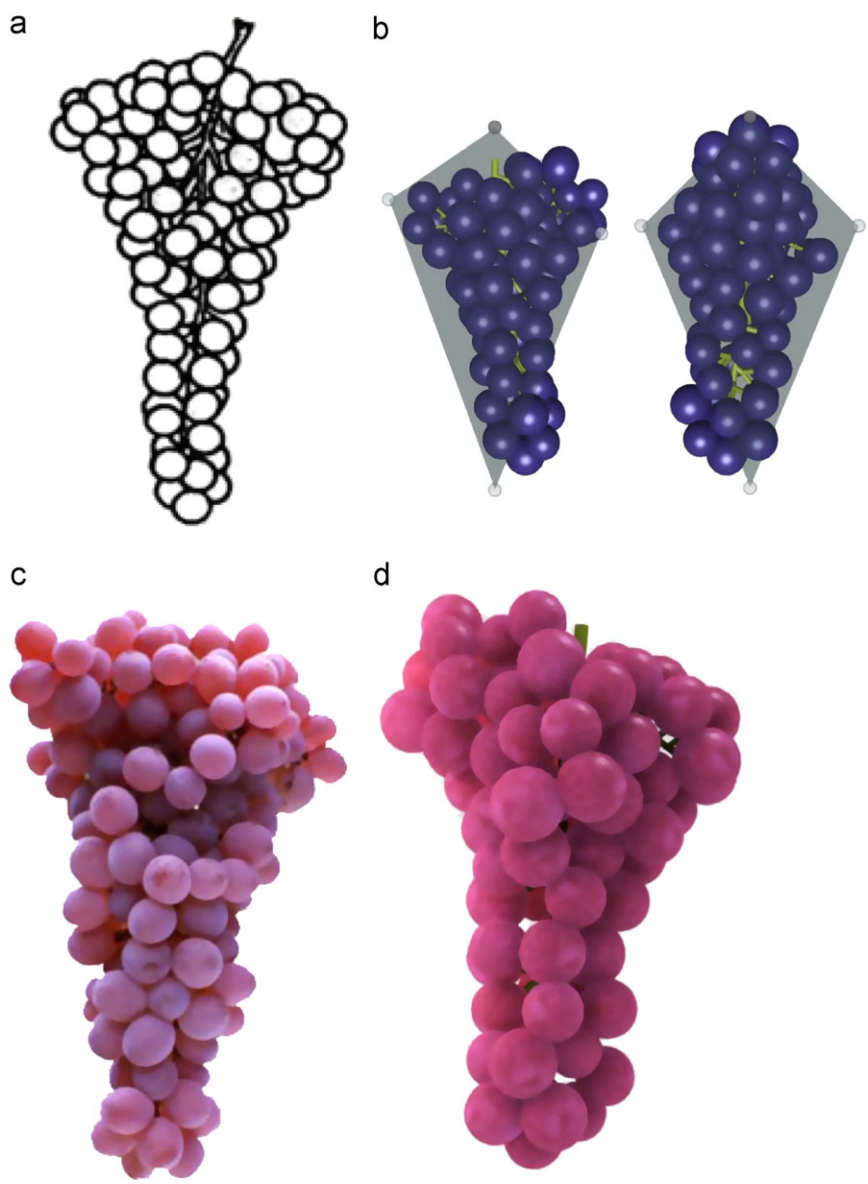

Fig. 11. Long conical of grape bunch. (a) Sample shape illustration, (b) front and side views of the shape control result, (c) real grape bunch and (d) rendered result.

$n_1 \ldots n_{m-1}$: number of derivation steps for first-order axes.

#define l_i 60 /* internode's initial length */
#define $\mathbf{l_w}$ 10 /* **internode's length after withering** */
#define r_l 1 /* internode's length decreasing rate */
#define r_r 0.75 /* the ratio of sphere's radius to internode's initial length */
#define α 45 /* yaw angle */

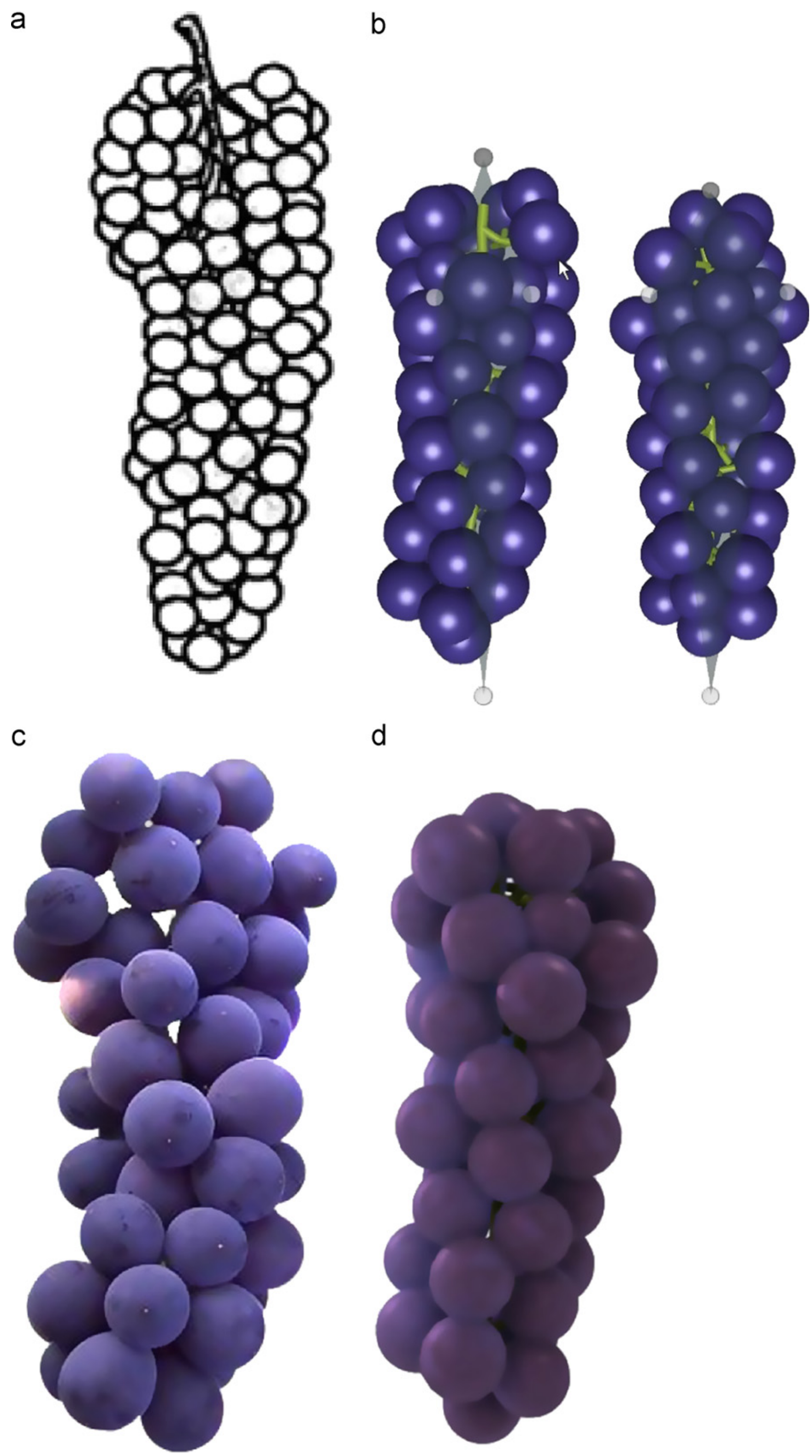

Fig. 12. Cylindrical of grape bunch. (a) Sample shape illustration, (b) front and side views of the shape control result, (c) real grape bunch and (d) rendered result.

$\omega : A_r(m,l_i)$
$p_1 : A_r(i,j) : i>1$
$\quad \rightarrow ?\boldsymbol{E}(\mathbf{0},\mathbf{0},\boldsymbol{l})[//A_r(i-1,j*r_l)][+(\alpha)A_f(n_{i-1},j*r_l)]$
$p_2 : A_r(i,j) : i==1$
$\quad \rightarrow A_e(j*r_l)$
$p_3 : A_f(i,j) : i>1$
$\quad \rightarrow ?\boldsymbol{E}(\mathbf{0},\mathbf{0},\boldsymbol{l})[//A_f(i-1,j*r_l)][+(\alpha)A_e(j*r_l)]$
$p_4 : A_f(i,j) : i==1$
$\quad \rightarrow A_e(j*r_l)$
$p_5 : A_e(i)$
$\quad \rightarrow ?\boldsymbol{E}(\mathbf{0},\mathbf{0},\boldsymbol{l})[A_p(i*r_l)][+(\alpha)A_p(i*r_l)][-(\alpha)A_p(i*r_l)]$
$p_6 : A_p(i)$
$\quad \rightarrow ?\boldsymbol{E}(\mathbf{1},\mathbf{0},\boldsymbol{l})S(l*r_r)$
$\mathbf{p_7} :? \quad \boldsymbol{E}(\boldsymbol{type},\theta,\boldsymbol{l}) : \boldsymbol{type}==\mathbf{0}$
$\quad \rightarrow +(\boldsymbol{\theta})!(\boldsymbol{w})\boldsymbol{F}(\boldsymbol{l})$
$\boldsymbol{p_8} :? \quad \boldsymbol{E}(\boldsymbol{type},\theta,\boldsymbol{l}) : \boldsymbol{type}==\mathbf{1}\&\&\boldsymbol{l}==\boldsymbol{l_w}$
$\quad \rightarrow +(\theta)!(\boldsymbol{w})\boldsymbol{F}(\boldsymbol{l})\%$
$\boldsymbol{p_9} :? \quad \boldsymbol{E}(\mathbf{type},\theta,\boldsymbol{l}) : \boldsymbol{type}==\mathbf{1}\&\&\boldsymbol{l}!=\boldsymbol{l_w}$
$\quad \rightarrow +(\boldsymbol{\theta})!(\boldsymbol{w})\boldsymbol{F}(\boldsymbol{l})\boldsymbol{S}(\boldsymbol{l_i}*\boldsymbol{r_r})$

For the rules p_1–p_6, the line drawing command $F()$ is replaced by a *communication module* $?E()$ to send and retrieve information for the interaction simulation process to adjust the growing direction of the internode. The newly added rules, p_7, p_8, and p_9, correspond to the *communication module* that used to deal with the environment for adjusting the growing direction of the internode. The *type* parameter represents the growing of an internode (*type*=0) or a pedicel which is followed by a berry (*type*=1). Rule p_8 is used to deal with withering the pedicel and the berry if the environment is too crowded to grow a berry. θ and l are the output of the *communication module* representing the growing direction and the length of the internode after adjustment.

Interaction mechanism: When a newborn internode is going to be derived, its growing space is checked to see if the space is

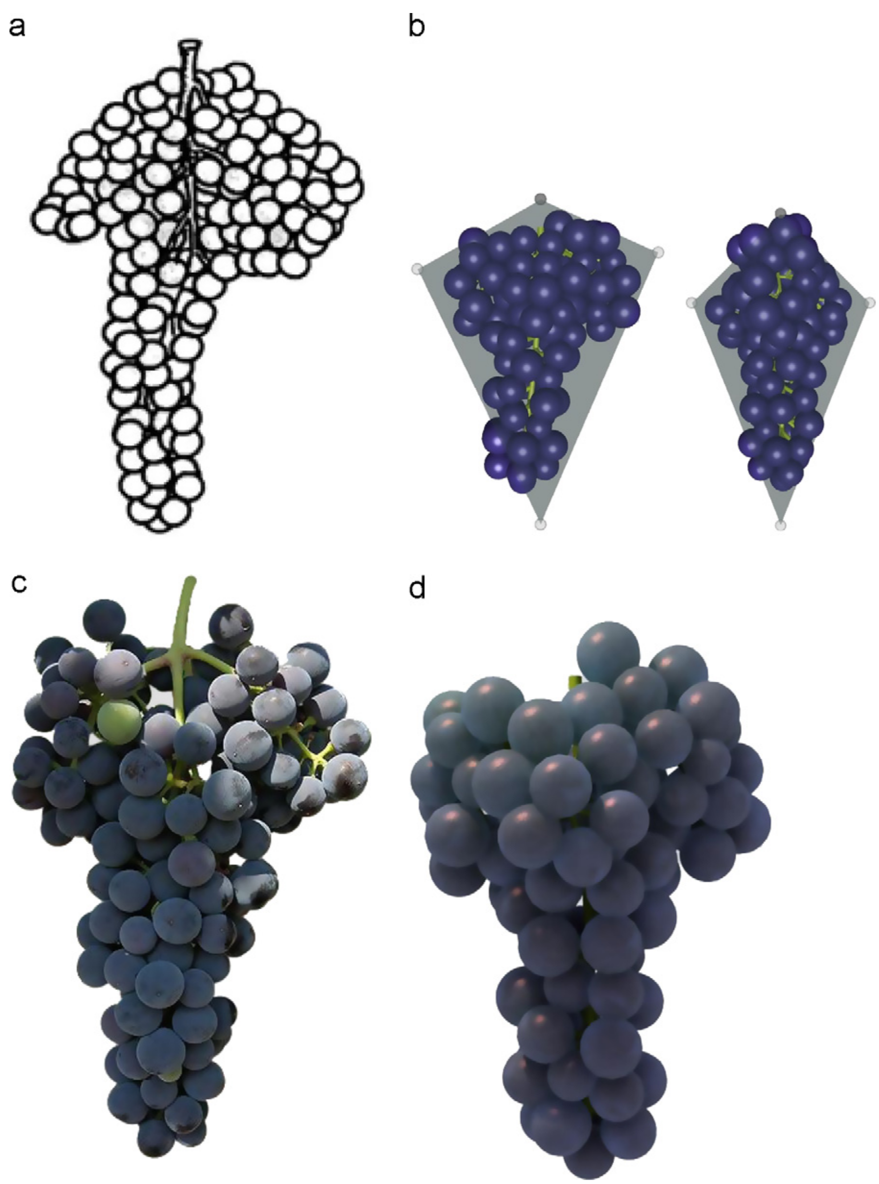

Fig. 13. Winged cylindrical of grape bunch. (a) Sample shape illustration, (b) front and side views of the shape control result, (c) real grape bunch and (d) rendered result.

available for it to grow using the interaction simulation process. The interaction simulation probes the space by performing collision detections between the newborn internode and the current structure of the grape bunch. The tip of a newborn internode is attached with a sphere with the predefined berry's radius b_r if the internode is a pedicel, or with the predefined internode's radius r_s ($r_s \ll b_r$) otherwise. Additionally, the current structure, represents the environment, consists of the spheres of all existing internodes.

If there are any collisions between the sphere and the current structure, the pushing force $\vec{F}$ will then be computed to rotate the growing direction of the newborn internode.

Let the current structure O be a set of spheres o_j centered at c_j which intersects with the sphere s of a newborn internode i. The pushing force $\vec{F}$ is the average of the summation of the approximated repelling forces and is computed by

$$\vec{F} = \frac{1}{n}\sum_{j=1}^{n}\left(\vec{v_j} * \frac{d_j}{R}\right) \tag{1}$$

where n is the cardinality of O, $\|O\|$, $\vec{v_j}$ is the normalized vector of $\overrightarrow{o_j s}$, d_j is the overlapping distance between s and o_j, and R is the diameter of s. An illustration for the pushing force can be seen in Fig. 7. The rotation angles θ and ϕ around L-axis (symbol $+$) and U-axis (symbol &) are then computed by

$$\begin{cases} \theta = \vec{F_L} * \delta \\ \phi = \vec{F_U} * \delta \end{cases} \tag{2}$$

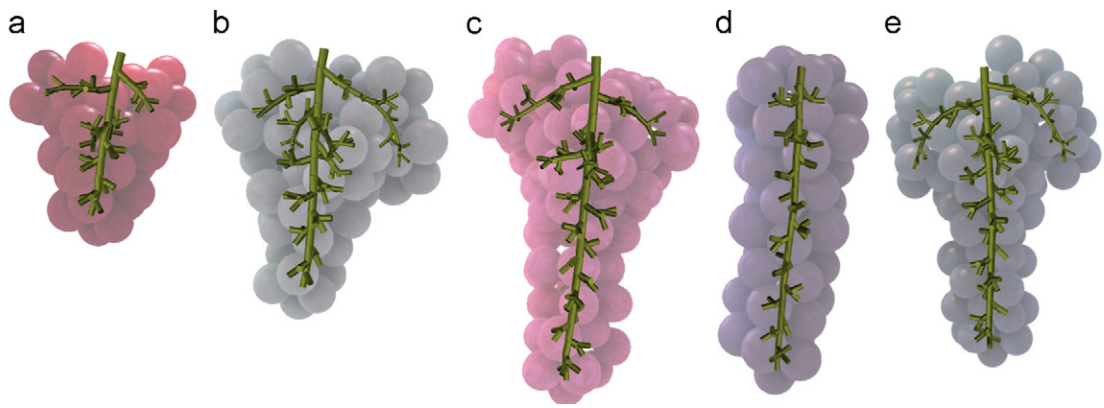

Fig. 14. The underneath internode structure of the results above. (a) Short conical, (b) shouldered conical, (c) long conical, (d) cylindrical and (e) winged cylindrical.

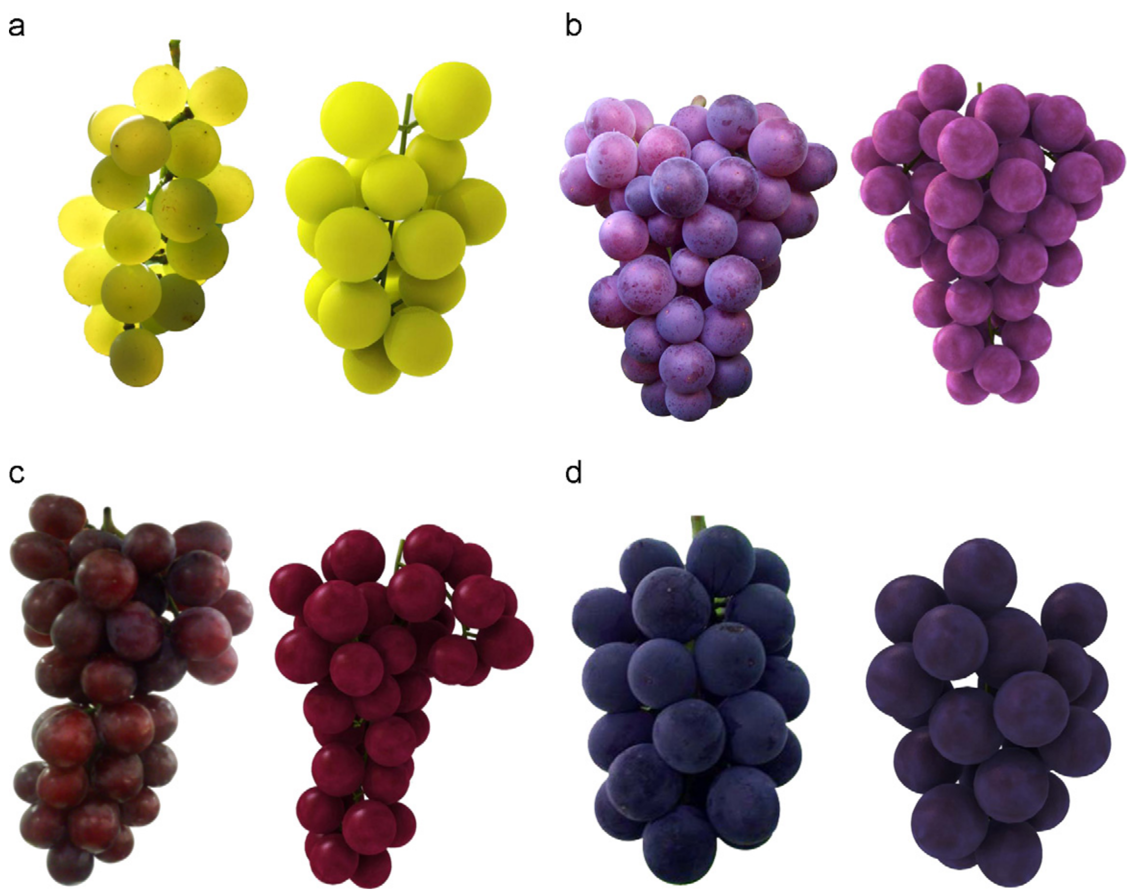

Fig. 15. More results of rendered grape bunches (right) compared to the real ones (left).

respectively, where δ represents the accumulation threshold of the total rotation angle that limits the adjustment range of the growing direction.

The newborn internode $\hat{i}$ is now rotated by $+(\theta)$ and $\&(\phi)$, and the collision detection follows again. The stop criterion for this adjustment is by limiting the number of adjustments and accumulated rotation angle; namely, when the accumulated rotation angle reaches δ, or the number of adjustments reaches t. If we do not find a suitable angle for an internode, we set the length of the internode to zero and discard the following growth from this internode. Note that if the newborn internode represents a pedicel, only t is applied.

Table 3
Input parameters used for modeling all results.

			p_3				p_4				p_5				p_6			
Fig.	l	m	w	r	n_{m-1}	r_d	w	r	n_{m-1}	r_d	w	r	n_{m-1}	r_d	w	r	n_{m-1}	r_d
13	253	9	79	76	3	4	116	91	5	6	101	112	4	8	97	103	4	8
14	377	13	190	130	8	7	110	150	4	9	150	150	6	10	150	150	6	11
15	512	18	150	150	6	8	150	102	6	7	150	150	6	10	150	150	6	11
16	523	18	47	133	2	7	47	136	2	9	80	105	3	8	63	108	3	9
17	525	18	190	86	8	5	199	113	8	7	150	150	6	10	150	150	6	11
18(a)	267	9	47	18	2	1	51	35	2	3	71	45	3	5	83	52	3	6
18(b)	377	13	167	85	7	5	182	84	7	6	202	78	8	6	214	72	9	7
18(c)	461	16	202	63	8	4	135	89	5	6	167	95	7	7	186	115	7	9
18(d)	272	9	64	217	3	8	43	243	2	8	57	218	2	8	78	204	3	8
19(a)	528	18	9	17	0	1	10	19	0	2	10	17	0	3	9	16	0	4
19(b)	122	4	10	17	0	1	8	17	0	2	10	19	0	3	9	22	0	3
19(c)	65	2	42	33	2	1	52	33	2	1	43	51	2	1	44	48	2	1
19(d)	243	8	127	79	5	4	111	56	4	4	132	56	5	5	134	73	5	7
19(e)	477	16	10	16	0	1	8	19	0	2	9	15	0	3	11	15	0	4

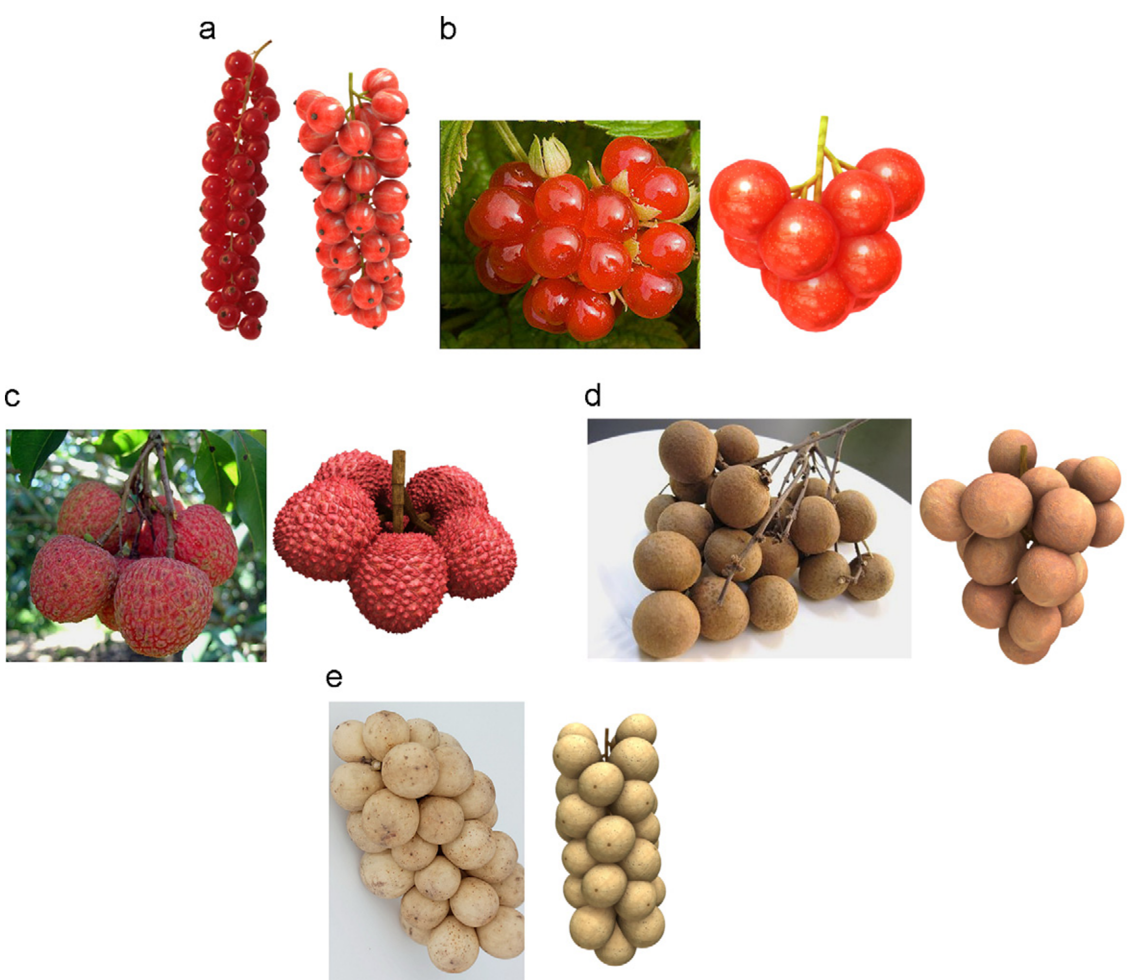

Fig. 16. More variant results of panicle berry bunches (right) as compared to the real one (left): (a) Redcurrant, (b) rubus, (c) lychee, (d) longan and (e) duku.

To take gravity into account, we simply adjust the newborn internode downward if there is no collision. Trivially, if the collision occurs after adjusting downward, the adjustment proceeds.

If the newborn internode represents a pedicel and the adjustment fails, the internode will be withered. The length of this internode will be shortened to l_w and the growth of the following berry will be canceled to simulate the thinning. Otherwise, the sphere s of the newborn internode $\hat{i}$ will be merged into the current structure.

4.3.3. Geometry detail

The following L-system 3 shows the final version of our proposed open L-system that grows grape bunches in 3D.

A_{r1}–A_{r4} are the first-order axes at right, left, front, and back respectively. In the previous L-systems, the length of every internode is the same due to the length decreasing rate r_l being equal to 1. In fact, branches of lower order are thinner and shorter than branches of higher order (assuming a Horton–Strahler order) over the branching hierarchy. Thus, r_{rr}, r_{rf}, r_e, r_{ff}, and r_p are set to be different decreasing rates for the different axes/branches. Furthermore, the diameter of the internode will be getting thinner with r_w. Besides, the function $RND(x)$ is used to pick an integer between the given range x of uniform statistical distribution for the berries' radius b_r rather than keeping them in the same size.

L-system 3. The complete L-system of a grape bunch.

Input
m : number of derivation steps for rachis.
$n_1 \ldots n_{m-1}$: number of derivation steps for first-order axes.

#define l_i 50 /* internode's initial length */
#define l_w 10 /* internode's length after withering*/
#define w_i 15 /* internode's initial width */
#define r_w 0.98 /* internode's diameter decreasing rate */
#define r_{rr} 0.99 /* internode's length decreasing rate (rachis to rachis)*/
#define r_{rf} 0.89 /* internode's length decreasing rate (rachis to first-order axis) */
#define r_e 0.6 /* internode's length decreasing rate (for end structure) */
#define r_{ff} 0.99 /* internode's length decreasing rate (first-order axis to first-order axis) */
#define r_p 1.5 /* internode's length decreasing rate (for pedicel) */
#define rg $[\frac{l_i - l_i}{10}, \frac{l_i + l_i}{10}]$ /* range of berry's radius */
#define α_y 60 /* yaw angle */
#define α_r 120 /* roll angle for pedicel */

$\omega : A_{r1}(m,l_i,w_i)$
$p_1 : A_{r1}(i,l,w) : i>1 \rightarrow ?E(0,0,0,l,w)[//A_{r2}(i-1,l*r_{rr})][+(\alpha_y) A_f(n_{i-1},l*r_{rf})]$
$p_2 : A_{r2}(i,l,w) : i>1 \rightarrow ?E(0,0,0,l,w)[/A_{r3}(i-1,l*r_{rr})][+(\alpha_y) A_f(n_{i-1},l*r_{rf})]$
$p_3 : A_{r3}(i,l,w) : i>1 \rightarrow ?E(0,0,0,l,w)[//A_{r4}(i-1,l*r_{rr})][+(\alpha_y) A_f(n_{i-1},l*r_{rf})]$
$p_4 : A_{r4}(i,l,w) : i>1 \rightarrow ?E(0,0,0,l,w)[\backslash A_{r1}(i-1,l*r_{rr})][+(\alpha_y) A_f(n_i V1,l*r_{rf})]$
$p_5 : A_{r1\ldots4}(i,l,w) : i==1 \rightarrow A_e(l*r_e,w)$
$p_6 : A_f(i,l,w) : i>1 \rightarrow ?E(0,0,0,l,w)[\backslash A_f(i-1,l*r_ff)][+(\alpha_y)A_e(l*r_e,w)]$
$p_7 : A_f(i,l,w) : i==1 \rightarrow A_e(l*r_e,w)$
$p_8 : A_e(l,w) \rightarrow ?E(0,0,0,l,w)[A_p(l*r_p)][+(\alpha_y)/(\alpha_r)A_p(l*r_p)][-(\alpha_y)\backslash(\alpha_r) A_p(l*r_p,w)]$
$p_9 : A_p(l,w) \rightarrow ?E(1,0,0,l,w)$
$p_{10} : ?E(type,\theta,\phi,l,w) : type==0 \rightarrow +(\theta)\&(\phi)\ !(w*r_w)F(l)$
$p_{11} : ?E(type,\theta,\phi,l,w) : type==1 \&\& l==l_w \rightarrow +(\theta)\&(\phi)!(w*r_w)F(l)\%$
$p_{12} : ?E(type,\theta,\phi,l,w) : type==1 \&\& l!=l_w \rightarrow +(\theta)\&(\phi)!(w*r_w)F(l)S(RND(rg))$

5. Results

The proposed approach is implemented by C++ with DirectX 9.0 API on a personal computer of Intel Core i5-3470 3.2 GHz, 4 GB system memory, with nVIDIA GeForce GTX 550 Ti 1 GB video memory, running Windows 7 SP1. In our implementation, we set $C_l=29.0$, $C_w=25.0$ and $C_r=0.056$ for a 600∗600 interaction window.

In the following experiments, the L-system 3 is used with the accumulated rotation angle $\delta=15$ and the number of adjustments $t=50$ in the interaction simulation. Fig. 8 shows the user interface. View control buttons at the upper left of the UI allow users to switch the views of the front and the side. Export button allows users to export the model to .OBJ file format for further processing.

Table 2 gives the execution times for different numbers of internodes and berries. The more internodes and berries a bunch have the more computational time is required to process the collisions between the spheres.

Figs. 9, 10, 11, 12 and 13 show the modeling results by L-system 3. All grape bunch models were interactively constructed and exported by our method, and rendered in MAYA with subsurface scattering as compared with the corresponding real grape bunch. Fig. 9 demonstrates the short conical of grape bunch, where (a) presents a sample illustration of this type, (b) shows the front view and side view of the modeling grape bunch, and (c) displays a photograph of a real grape bunch of this type as compared with our rendered result (d). To model this type of grape bunch, the distance between control point p_1 and p_2 should not be too long, and the positions of side control points should not be too high with almost the same horizontal distance to the p_1.

Fig. 10 demonstrates the shouldered conical type that one of the side control points is far from the center while the other is relatively close when modeling this type of bunch. Fig. 11 shows the long conical type. The difference between this type and the short conical type (Fig. 9) is the length of the rachis, i.e., the distance between p_1 and p_2. Fig. 12 presents the cylindrical type where the positions of the side control points are very close to model the cylindrical shape of the bunch. The winged cylindrical type is shown in Fig. 13 with one of the side control points far from the center and the other relatively close at the front view. The double bunch winged type is not shown because it can be separated into two single bunches. The underneath internode structure of the above grape bunches is shown in Fig. 14. Moreover, Fig. 15 shows the flexibility and effectiveness of our method by modeling several variant grape bunches and comparing them with real corresponding pictures of grape bunches. The input parameters and constants l, w, r, m, n_{m-1} and r_d of all results are shown in Table 3.

Furthermore, our proposed approach can be extended to model several kinds of berry bunch with panicle inflorescence. Fig. 16 shows berry bunches of (a) redcurrant, (b) rubus, (c) lychee, (d) longan and (e) duku respectively. Due to the fact that the inflorescences of these fruits are panicle, they can be modeled using L-system 3. Currant and duku are similar to the cylindrical type of the grape bunch; thus the side control points should be adjusted near center. The other three bunches are similar to the short conical type, so shortening the distance between the p_1 and p_2 will result in berry bunches of this kind.

6. Conclusions and future work

We have proposed a grammar-based approach using an open L-system for grape bunches modeling. The derived formal rules are general for modeling almost all types of grape bunches. The proposed user interface for the development control is intuitive and effective. Based on users' profiled shape of a grape bunch, fundamental parameters obtained are used to determine all parameters of the open L-system. Finally, when interpreting the generated string for growing the grape bunch, the interaction simulation process simulates the environment interactions via a *communication module* for the adjustment of growing directions of newborn internodes and natural effects of thinning of berries. Our approach is not only general for modeling grape bunches, but also can be extended to modeling of variant panicle berry bunches.

In the future, we would like to deform the berry surface to have more realistic berries as a result of environment interactions instead of using spheres. More parameters, such as sunlight and the nutrition of the berries, can be considered to improve the realism of the bunch . We would also like to use the proposed approach for modeling the evolution of the grape bunch's growth and maturation in the form of evolutionary animation. The material of the berry is crucial for realistic rendering and is worth devoting time for the rendering of grape bunches. Furthermore, the extension of the proposed L-system is worth exploring, such as adjusting the length of the pedicel to well model the lychee and longan.

Appendix A. Supplementary material

Supplementary data associated with this article can be found in the online version of http://dx.doi.org/10.1016/j.cag.2013.01.002.

References

[1] Prusinkiewicz P, Lindenmayer A. The algorithmic beauty of plants. Heidelberg, Berlin, Germany: Springer-Verlag; 1990.
[2] Müller P, Wonka P, Haegler S, Ulmer A, Van Gool L. Procedural modeling of buildings. In: Proceedings of SIGGRAPH 2006. 2006, p. 614–23. http://dx.doi.org/10.1145/1141911.1141931.
[3] Gagnon J, Paquette E. Procedural and interactive icicle modeling. The Visual Computer: International Journal of Computer Graphics 2011;27(6–8): 451–61. http://dx.doi.org/10.1007/s00371-011-0584-9.
[4] Beneš B, Šťava O, Měch R, Miller G. Guided procedural modeling. In: Computer graphics forum, vol. 2. 2011. p. 325–34. http://dx.doi.org/10.1111/j.1467-8659.2011.01886.x.
[5] Food & Agriculture Organization (FAO). Statistical data of food and agricultural commodities production (August Accessed on 2 August 2011). URL ⟨http://faostat.fao.org/site/339/default.aspx⟩.
[6] Měch R, Prusinkiewicz P. Visual models of plants interacting with their environment. In: The 23rd annual conference on computer graphics and interactive techniques. ACM, New York, NY, USA; 1996. http://dx.doi.org/10.1145/237170.237279.
[7] Palubicki W, Horei K, Longay S, Runions A, Lane B, Měch R, et al. Self-organizing tree models for image synthesis, ACM Transactions on Graphics (TOG). http://dx.doi.org/10.1145/1531326.1531364.
[8] Prusinkiewicz P, James M, Měch R. Synthetic topiary. In: Proceedings of SIGGRAPH 1994. 1994. p. 351–58. http://dx.doi.org/10.1.1.23.6719.
[9] Prusinkiewicz P. Graphical applications of l-systems. In: Graphics interface '86. 1986. p. 247–53.
[10] Ebert DS, Musgrave FK, Peachey D, Perlin K, Worley S. Texturing & modeling, Morgan Kaufmann. Waltham, Massachusetts, United States: Elsevier; 2003.
[11] Deussen O, Hanrahan P, Lintermann B, Měch R, Pharr M, Prusinkiewicz P. Realistic modeling and rendering of plant ecosystems. In: Proceedings of SIGGRAPH 1998. 1998. p. 275–86.
[12] Prusinkiewicz P, Hammel M. A fractal model of mountains with rivers. In: Graphics interface '93, vol. 4. 1993. p. 174–80.
[13] Dai W-K, Shih Z-C, Chang R-C. Synthesizing feather textures in galliformes. In: Computer graphics forum, vol. 14(3). 1995. p. 407–20.
[14] Chen Y, Xu Y, Guo B, Shum H-Y. Modeling and rendering of realistic feathers. In: Proceedings of SIGGRAPH 2002. 2002. p. 630–6. http://dx.doi.acm.org/10.1145/566654.566628.
[15] Parish Y, Müller P. Procedural modeling of cities. In: The 28th annual conference on computer graphics and interactive techniques. 2001. p. 301–8. http://dx.doi.acm.org/10.1145/383259.383292.
[16] Hanan J. Parametric l-systems and their application to the modeling and visualization of plants. PhD thesis. University of Regina; 1992.
[17] Prusinkiewicz P, Hammel H, Hanan J, Měch R. Visual models of plant development. Handbook of Formal Languages. doi:10.1.1.23.8332.
[18] Prusinkiewicz P, Hammel M, Měch R, Hanan J. The artificial life of plants. In: SIGGRAPH '95 course notes, vol. 7. 1995. p. 1–38.
[19] Jirasek C, Prusinkiewicz P, Moulia B. Integrating biomechanics into developmental plant models expressed using l-systems. In: Plant biomechanics 2000, proceedings of the 3rd plant biomechanics conference. Stuttgart: Georg Thieme Verlag; 2000. p. 615–24.
[20] Prusinkiewicz P, Muendermann L, Karwowski R, Lane B. The use of positional information in the modeling of plants. In: Proceedings of SIGGRAPH 2001. Los Angeles, California; 2001. p. 289–300.
[21] Rombough L. The grape grower: a guide to organic viticulture, Chelsea Green, Vermont, United States; 2002.
[22] Scott T. Concise encyclopedia biology. Berlin, Germany: Walter de Gruyter; 1996.
[23] Wikipedia, Grape (July 8, July 2011). URL ⟨http://zh.wikipedia.org/wiki/%E8%91%A1%E8%90%84⟩.
[24] Wikipedia, Inflorescence (July 8, July 2011). URL ⟨http://en.wikipedia.org/wiki/Inflorescence⟩.
[25] Wikipedia, Panicle (July, Accessed on 8 July 2011). URL ⟨http://en.wikipedia.org/wiki/Panicle⟩.
[26] Chinese-Plant, Dealing with the claspers, inflorescence, and berries when trimming a grape (June 25, June 2011). URL ⟨http://www.chinese-plant.com/yuanyi/08-11/5012.htm⟩.
[27] Guan Z-X, Chao W-J, Miu K, Yao L-Q. Study on the characteristic of flowering biology of red globe. Sino-overseas Grapevine & Wine. doi:1004-7360.0.2004-06-006.
[28] Weaver R. Grape growing. Hoboken, New Jersey, United States: John Wiley and Sons; 1976.
[29] Simpson M. Plant systematics. Amsterdam, Netherlands: Academic Press, Elsevier; 2006.